Journal of Geointerface, Vol. 3, No. 2, December 2024, pp. 79–92 e-ISSN: 2583-6900

Mineralogy of carbonatite-breccia: Amba Dongar carbonatite diatreme, Gujarat, India

Jan Schulzki[1], Shrinivas G. Viladkar [2,*], Helmut Schleicher [1]

[1] *Mineralogisch-Petrographisches Institute, Hamburg Universität, Grindelallee 48, Hamburg, Germany*
[2] *Carbonatite Research Centre, Amba Dongar, Kadipani, Gujarat 390117, India*

ABSTRACT

Carbonatite-breccia forms a major unit in the carbonatite-alkaline diatreme of the Amba Dongar carbonatite ring complex. In addition to the innermost part of the ring structure, small and large plugs outside the ring structure are also formed in the form of discontinuous rings around the sövite. It mainly comprises rounded to sub-angular fragments of basement metamorphics, Bagh sandstones, pre-carbonatite basalt, nephelinite and sövite set in the carbonatitic matrix. Besides rock fragments, it also shows the presence of xenocrystal minerals. Carbonatite breccia is later invaded by sövite, alvikite and ankeritic carbonatite. Thorite, pyrochlore, barite, apatite, fluorite and REE-minerals were introduced in carbonatite breccia by these later intrusives. The zircon, however, seems to have been caught up from metamorphic gneisses. Microprobe analyses of all these minerals in the carbonatite-breccia indicate the presence of important REEs. Carbonatite breccia has been silicified in places by invading hydrothermal solutions rich in fluorite and silica.

ARTICLE HISTORY

Received 2 November 2024
Revised 25 November 2024
Accepted 29 November 2024

https://doi.org/10.5281/zenodo.14252287

KEYWORDS

carbonatite breccia
Amba Dongar carbonatite ring complex
sövite
Bagh sandstone
apatite
fluorite
pyrochlore
REE
hydrothermal solution

Editorial handling

R. Radhika
University of Kerala, India

1. Introduction

Carbonatite-breccia forms a major unit of the Amba Dongar diatreme. However, such an important unit of this diatreme has not been subjected to detailed investigation so far. This study aims to investigate the mineralogy, petrography and geochemistry of the carbonatite-breccia unit of the Amba Dongar diatreme for the first time.

2. Geological setting of Amba Dongar

The Amba Dongar carbonatite-alkaline rock diatreme is located in the northwestern periphery of the Deccan basalt in the state of Gujarat. The carbonatite-alkaline rocks are emplaced into the Dharwar metamorphics, Bagh sedimentary beds and Deccan basalt sequences and the complex is situated in the deep fault zone of the Narmada River trending ENE that lies about 9 km south of the Amba Dongar carbonatite ring complex. The area is structurally highly disturbed and the main structural feature is the doming of the above-mentioned geological sequence which resulted inthe development of high-angle outward radially dipping sandstone from the central ring structure. The carbonatite activity began with the formation of a plug of 1.5 km diameter of the carbonatite-breccia in the central part of the ring structure. The detailed geological map of the study area with sample locations is given in Fig. 1.

In some places clear contact between the carbonatite-breccia and overlying pre-carbonatite basalts was identified (Fig. 2). While considering all newly exposed breccia along the road cuttings and in the valleys (collaring sövite) it is identified that the area of the original plug of breccia is much larger

*Corresponding author. Email: sviladkar@gmail.com (SGV), jan.schulzki@gmx.de (JS), Helmut.Schleicher@gmx.de (HS)

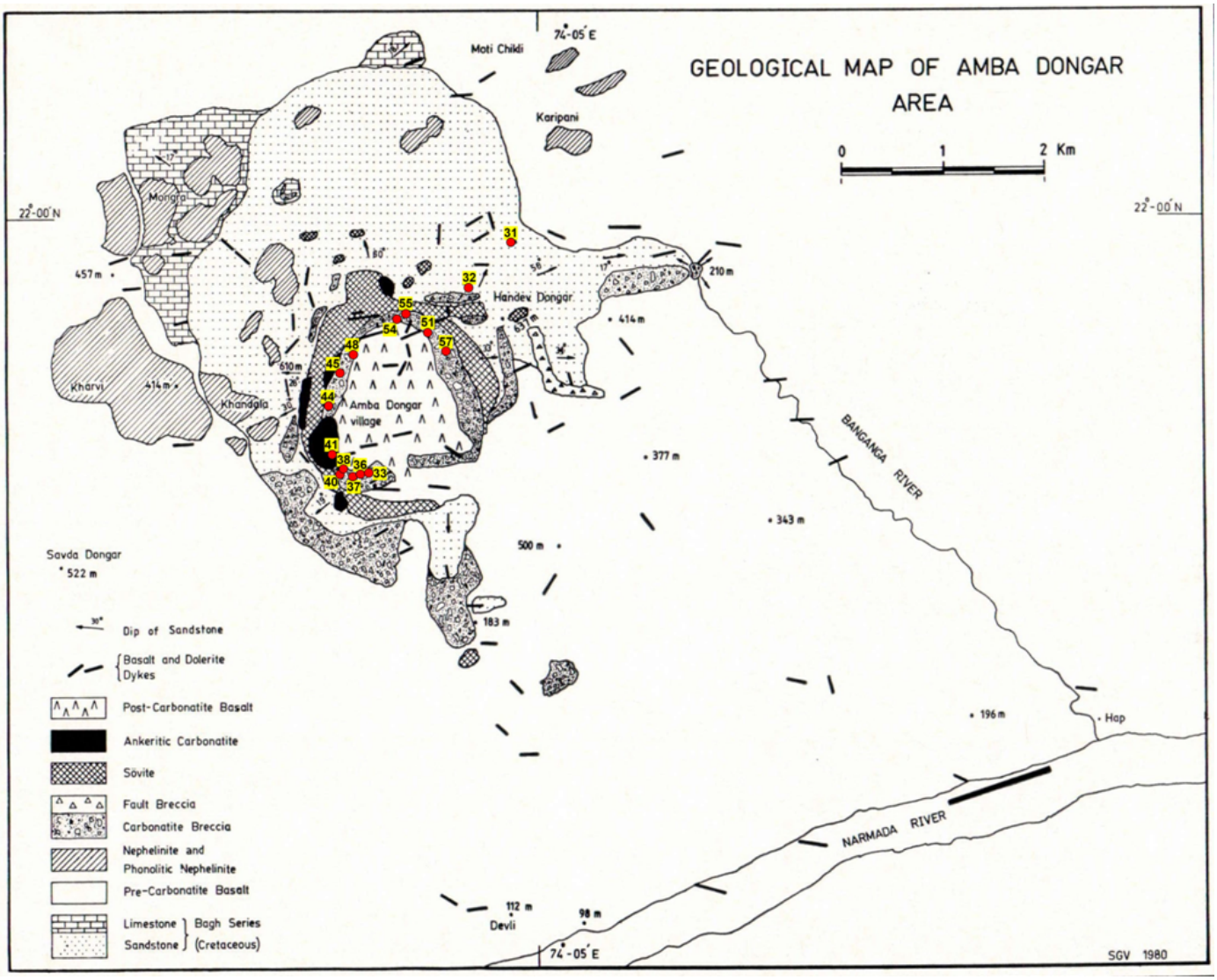

Fig. 1. Geological map of the study area with locations of samples along the inner rim carbonatite-breccia and the two plugs outside the inner rim.

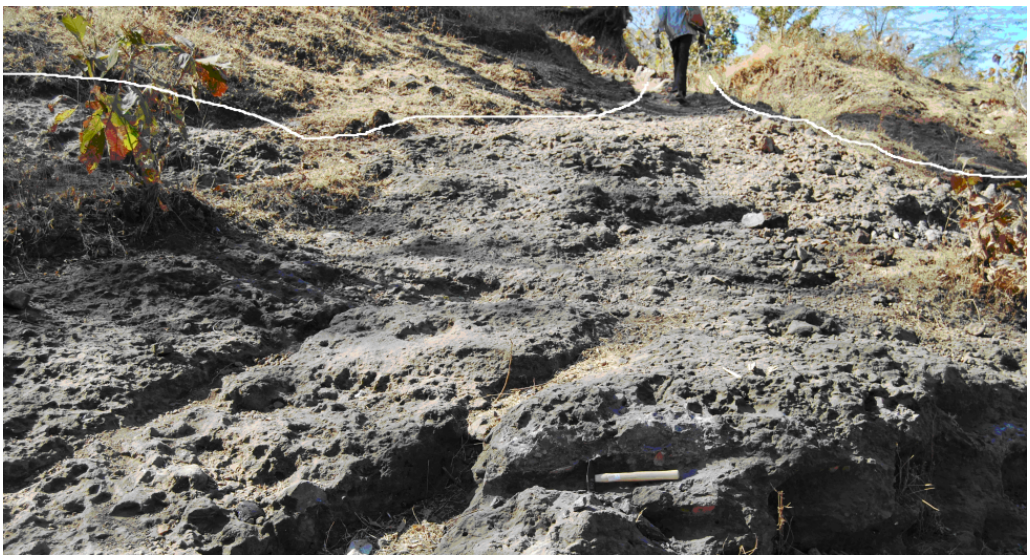

Fig. 2. Carbonatite-breccia exposure outside main inner rim, white lines indicate its contact with pre-carbonatite basalt.

Fig. 3. Inner rim carbonatite breccia with rounded to sub-angular fragments.

than 1.5 km. Generally, all breccia samples have large fragments of sövite, fenitized sandstone, alkaline rocks, basalts and metamorphic rocks such as slates and gneisses. The majority of sövite fragments in the breccia are rounded while fragments of all other rock units are sub-rounded (Fig. 3). The matrix is mostly carbonatite but at times it contains small amounts of silica.

3. Methodology

Various samples of carbonatite-breccia were petrographically studied and were selected for Philips XRF (PW 1450/20) analyses and mineral chemical analyses using electron microprobe (EMPA). Minerals were analysed using CAMECA SX 100 EPMA at the Mineralogisch-Petrographisches Institute, University of Hamburg, Hamburg. The microprobe was operated at an accelerating voltage of 15 kV and a beam current of 20 nA with a beam diameter of 1 µm. The various analytical conditions used for the analysis of thorite, zircon, barite, and apatite are given in the Appendix Table A–D.

4. Mineralogy and geochemistry of carbonatite-breccia

The whole rock element chemistry of fragments and matrix present in the carbonatite-breccia are given in Table 1. The whole rock analyses show the presence of a good amount of silica which could be due to the presence of silicate rock fragments. The high amount of Fe, Al and Mg in the matrix analyses of three rocks (40, 44 and 45) could be attributed to the presence of a few flakes of phlogopite/biotite in the carbonatitic matrix. Of the two carbonatite fragment analyses presented, one is composed of only calcite while the other has a good amount of barite along with calcite. The high Ba samples also show high SO_3 values in the analyses. A sample of sövite fragment and matrix shows very high CaF_2 content and both are impregnated by hydrothermal fluorite veins. Among the trace and rare earth element contents, Nb and LREE are conspicuously high. The high content of REEs could be attributed to the veins of ankeritic carbonatite in the sövite fragments and matrix.

4.1. Calcite

Calcite in sövite fragments occur as well-developed phenocrysts (Fig. 4A) and as absorbed crystals in an ankerite base (Fig. 4B). Sövite fragments are heavily impregnated by ankeritic carbonatite and show fragmental texture. All analysed carbonates are calcite with slight variations in contents of MgO and MnO. The Sr content is high in some fragments of calcite. Representative chemical analyses of carbonates in the carbonate-breccia are given

Table 1. Whole rock analyses of carbonatite breccia (fragments and matrix).

Sample	1	2	3	4	5	6	7
	31W	36 Fr	40M	44M	45M	51W	54 Fr
SiO_2	25.03	1.83	6.00	6.96	21.47	36.92	3.45
TiO_2	0.47	0.10	0.33	0.22	0.70	0.79	0.09
Al_2O_3	6.47	0.51	1.26	0.92	4.71	9.33	0.52
FeO	4.35	2.99	8.71	5.87	6.35	6.75	4.52
MnO	0.53	1.06	2.37	1.96	0.70	0.46	1.35
MgO	0.69	0.62	7.46	12.89	0.96	1.97	2.41
CaO	26.09	20.31	19.80	25.52	27.18	15.42	42.33
BaO	1.46	13.09	4.11	2.57	2.02	0.87	0.81
Na_2O	0.53	0.07	0.06	0.09	0.04	0.18	0.07
K_2O	3.72	0.08	0.14	0.16	1.25	6.25	0.07
P_2O_5	0.56	2.05	0.71	0.37	1.10	0.65	2.23
SO_3	0.45	7.60	1.53	0.00	1.01	0.24	0.24
CaF_2	3.73	15.18	16.18	4.87	1.58	2.43	1.78
LOI	23.67	17.73	24.59	34.52	25.85	16.26	34.67
Total	98.24	83.55	94.23	97.57	95.64	99.27	95.04
Co	3	0	2	5	8	12	7
Cr	0	0	0	0	16	11	0
Cu	13	0	0	0	26	17	16
Ga	7	2	0	0	3	14	0
La	1247	4882	3227	1606	1381	624	2025
Ce	1843	7160	5134	2871	2342	982	3907
Nd	502	1598	1312	782	691	272	1138
Ni	31	5	19	6	23	10	24
Pb	93	50	457	242	164	108	226
Rb	89	0	0	5	46	164	3
Sc	4	0	0	11	1	8	0
Sr	1969	1713	4234	4915	2292	1100	3266
Th	29	0	62	105	45	37	19
U	13	0	3	1	5	9	0
V	269	156	283	258	321	315	106
Y	82	114	151	173	120	72	385
Zn	223	192	755	595	322	289	771
Zr	142	0	0	0	167	297	557
Nb	274	73	479	235	874	419	703

W: whole rock analysis of breccia
M: Analysis of matrix
Fr: Analysis of fragment

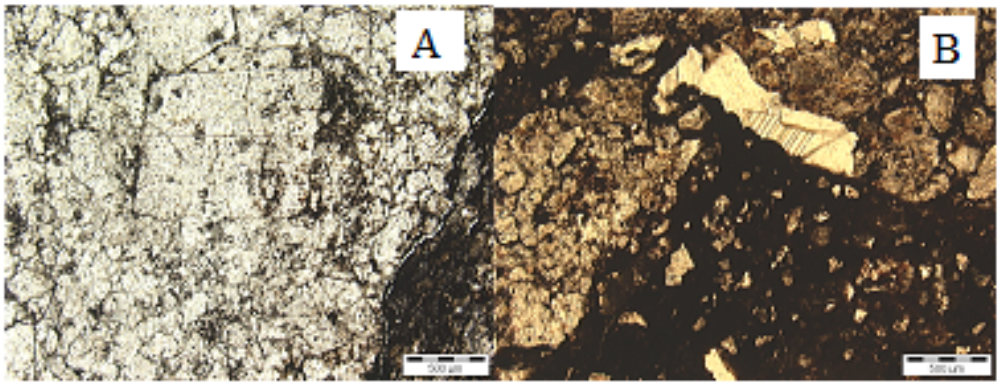

Fig. 4. A. Phenocryst of calcite in sovite fragment; B. Calcite crystals in ankeritic carbonatite base.

in Table 2.

4.2. Feldspar

Feldspar grains are dominantly formed either from fenite xenoliths or metamorphic protoliths. Since Sukheswala and Viladkar (1981) and Viladkar (1986, 1996) have given details of feldspars from fenites, these have not been analysed for this work. Feldspars from xenoliths of metamorphic protolith clearly show replacement texture at grain boundaries

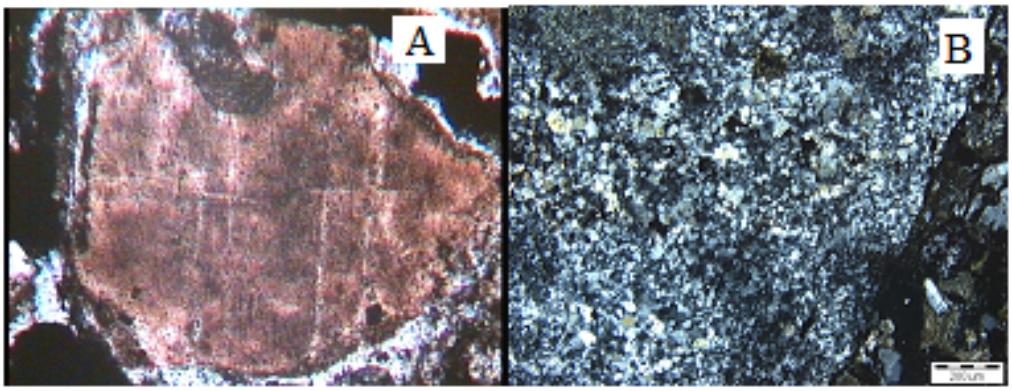

Fig. 5. A. Replacement of feldspar grain in metamorphic protolith, width 1 mm; B. Albitite fragment in carbonatite breccia.

Table 2. Analyses of carbonates from carbonatite breccia.

F	0.06	0.18	0.14	0.00	0.10	0.14
Na_2O	0.27	0.00	0.00	0.00	0.00	0.00
MgO	0.29	2.98	0.31	1.69	0.00	1.72
CaO	54.17	53.04	52.46	55.53	58.73	55.44
MnO	0.16	0.22	4.49	0.00	0.00	1.51
FeO	0.61	0.75	0.00	0.00	0.00	0.07
SrO	0.15	0.00	0.64	0.10	0.00	0.00
BaO	0.00	0.00	0.00	0.00	0.00	0.00
CO_2	44.28	42.61	41.96	42.68	41.17	41.12
Total	100.00	100.00	100.00	100.00	100.00	100.00

and albite fragments are also identified (Fig. 5A&B). The variation in chemical composition of feldspars in metamorphic protolith is depicted in Fig. 6.

4.3. Apatite

Apatite is found in the matrix of invading carbonatite and no idiomorphic crystals were found. Fluid inclusions are seen in the crystals. Back scattered electron (BSE) images of apatite with analysed points are shown in Fig. 7A&B. The analysed grains contain fluorine around 3.80% while the average Sr content is around 1.90%. The content of SiO_2 and REE show much variation and the plot of LREE against SiO_2 shows a positive correlation (Fig. 8). From apatite chemistry (Table 3) the apatite stoichiometry was calculated as

$$(Ca_{9.54}Na_{0.03}Sr_{0.19}SEE_{0.09})[(P_{5.94}Si_{0.14})O_4](F_{1.73}Cl_{0.002}OH_{0.27})$$

This shows that the analyzed apatite was fluor and strontium-apatite, with low contents of belovite and britholite. The F and Cl mapping of apatite grains shows a homogenous distribution of these elements throughout the grains. The Cl concentration is much less compared to F. This proves that the apatite is mainly fluor-apatite. Low Cl content of apatite analyses seems common in carbonatite apatites and according to Gittins (1989)'s observation, Cl goes into aqueous fluids associated with carbonatites. From the measurements and the resulting stoichiometric calculations, an average of 13.5% of ions are lacking on the X position. The missing 13.5% is assumed to be related to non-detectable OH^- anions. In general, the analysed apatite is closely similar to those reported by Doroshkevich et al. (2009).

4.4. Barite

Barite in different outcrops of breccias are mainly found within the matrix of invading carbonatite; either sövite or ankeritic carbonatite, and it does not show an idiomorphic shape like apatite. The mineral has almost 4.7% Sr (Table 4) which could be due to the celestine accommodated within the barite. In BSE images (Fig. 9) faint light and dark spots are visible and these may be due to the presence of celestine in parts. Both sövite and ankeritic carbonatite show good concentrations of barite in some samples, more so in the latter. We presume that barite is introduced in breccias during the invasion of sövite and ankeritic carbonatite melts.

4.5. Zircon

The zircons in carbonatite breccia are enclosed within the feldspars of the gneissic fragment (Fig. 10). Zircons have also been reported from carbonatites of Amba Dongar, however, no analysis has been reported so far. Two colour varieties of zircon are noticed and analysed; light brown and dark brown zircons. In the BSE image (Fig. 11) zircon crystals show slight alteration and the analyses reveal two

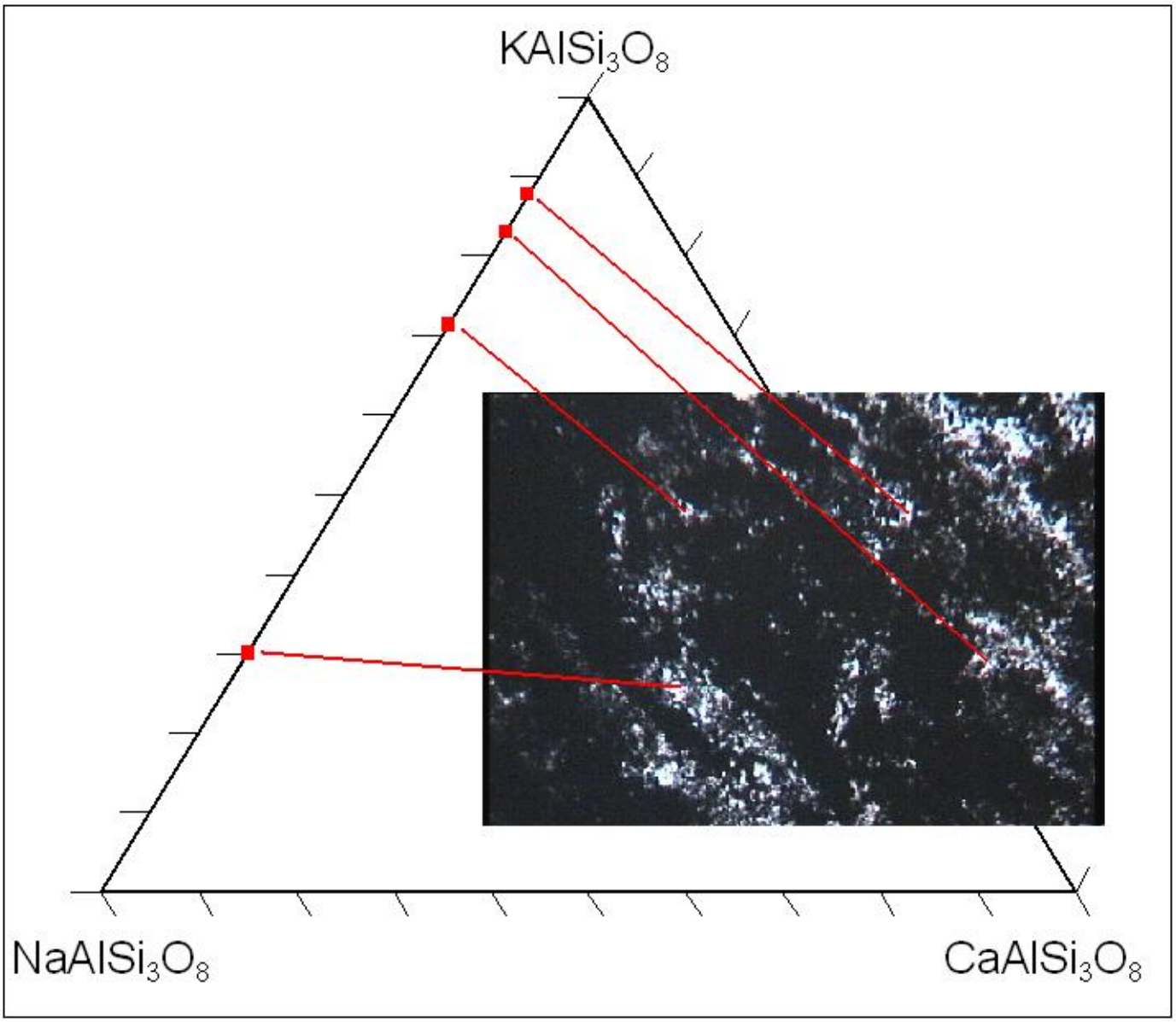

Fig. 6. Composition of feldspars (from a fragment of metasomatised metamorphic protolith) on feldspar triangle.

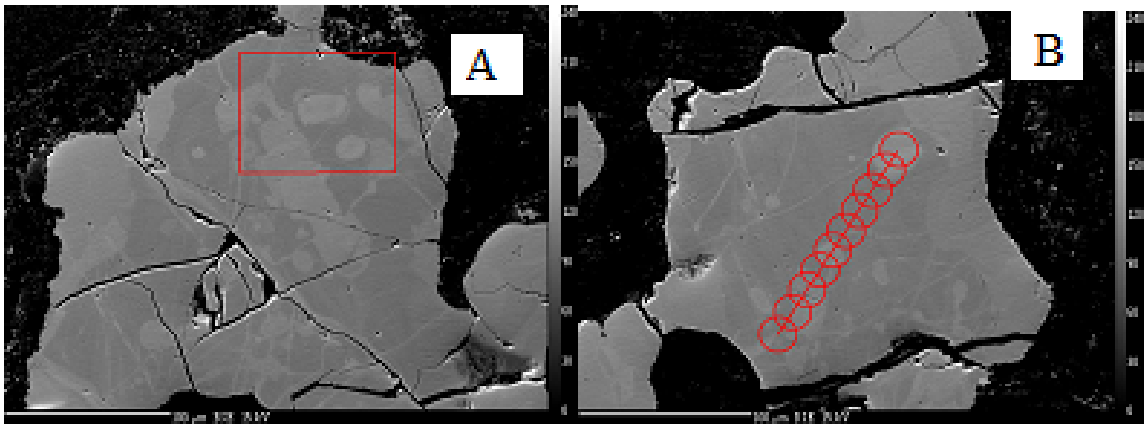

Fig. 7. A. BSE image of apatite; B. analysed points in a single line in an apatite crystal.

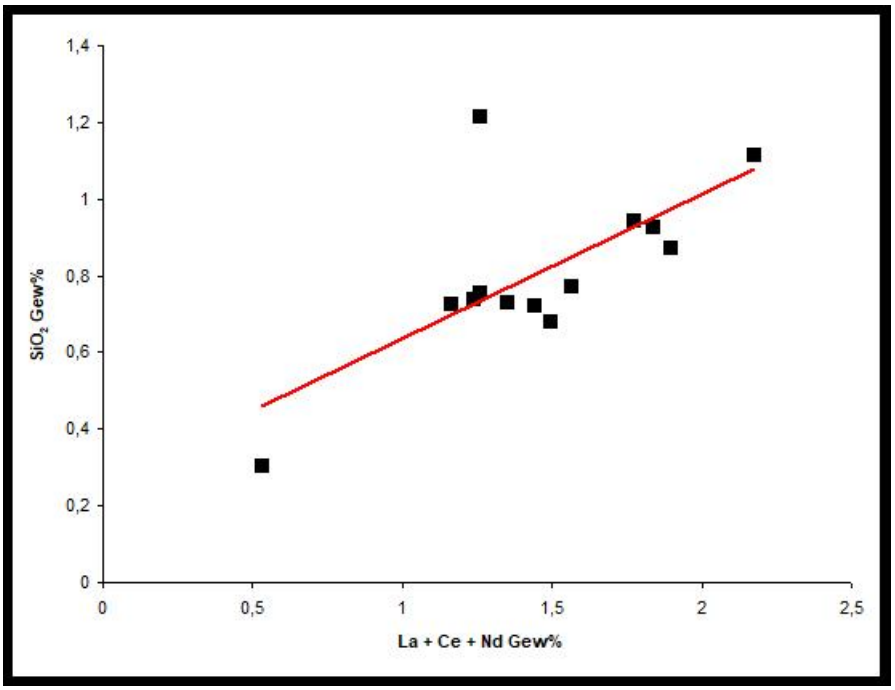

Fig. 8. SiO_2 vs LREE in apatites.

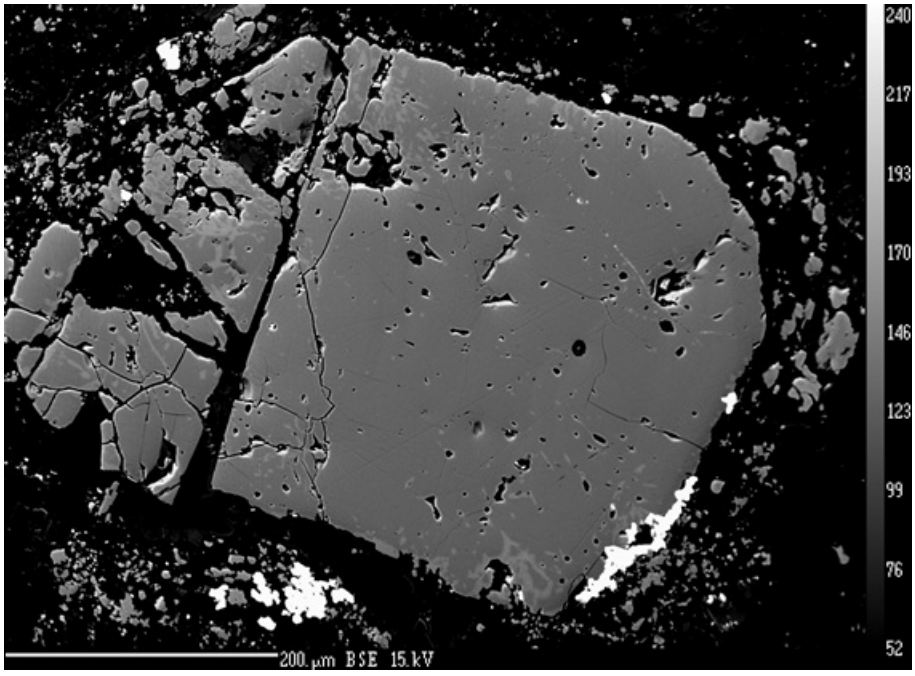

Fig. 9. BSE image of barite.

different phases which show different concentrations of Th and some other trace elements (Table 5). This alteration is similar to those described by Geisler et al. (2007) and this alteration perhaps is similar to metamictization.

4.6. Pyrochlore

Idiomorphic pyrochlore grains occur mainly in the xenoliths of sövites and alvikite intrusives in the carbonatite-breccia (Fig. 12), of which two grains were selected for EPMA. Both grains are nearly Ta-free calcio-pyrochlores. Both grains seem to have retained their primary composition with considerably high F, Ca and Na, otherwise, these are removed during alteration (Table 6). Slight fluctuation was observed in high field strength elements which may be due to fine primary zoning that is seen in pyrochlore (Fig. 13). Among all the elements, more pro-

Table 3. Analyses of apatite from carbonatite breccia.

F	3.144	3.076	3.388	3.279	3.242	3.237	3.271	3.233	3.272	3.278	3.328	3.191	3.172
Na_2O	0.099	0.064	0.166	0.066	0.076	0.099	0.085	0.092	0.067	0.064	0.069	0.080	0.093
MgO	0.000	0.000	0.000	0.000	0.000	0.000	0.000	0.000	0.000	0.000	0.000	0.000	0.000
Al_2O_3	0.000	0.007	0.000	0.000	0.000	0.000	0.000	0.000	0.000	0.000	0.000	0.000	0.000
SiO_2	1.218	0.683	0.307	0.732	0.774	0.943	0.722	0.872	0.741	0.757	0.727	0.927	1.114
$P2O_5$	40.255	40.895	42.335	41.490	41.576	41.354	41.907	41.612	41.900	41.984	41.865	41.361	40.907
Cl	0.010	0.006	0.010	0.007	0.008	0.006	0.006	0.006	0.007	0.007	0.006	0.006	0.006
K_2O	0.000	0.000	0.000	0.000	0.000	0.000	0.000	0.000	0.000	0.000	0.000	0.000	0.000
CaO	52.939	50.200	53.556	52.666	52.722	52.472	52.851	52.629	53.097	53.550	53.399	52.384	51.848
TiO_2	0.000	0.000	0.000	0.000	0.000	0.000	0.000	0.000	0.000	0.000	0.000	0.000	0.000
FeO	0.052	0.000	0.058	0.046	0.000	0.000	0.000	0.000	0.000	0.000	0.000	0.000	0.000
SrO	1.177	4.442	0.609	1.936	1.983	2.043	1.702	2.034	1.658	1.750	1.549	1.952	1.935
La_2O_3	0.444	0.554	0.130	0.427	0.491	0.563	0.435	0.599	0.393	0.400	0.369	0.578	0.670
Ce_2O_3	0.700	0.814	0.287	0.724	0.858	0.983	0.789	0.999	0.693	0.704	0.665	0.990	1.176
Pr_2O_3	0.000	0.000	0.000	0.032	0.000	0.000	0.000	0.044	0.000	0.000	0.000	0.033	0.041
Nd_2O_3	0.114	0.126	0.111	0.169	0.217	0.229	0.218	0.250	0.152	0.151	0.128	0.236	0.289
MnO	0.000	0.000	0.042	0.000	0.000	0.000	0.000	0.000	0.000	0.000	0.000	0.000	0.000
Total	100.170	100.912	101.044	101.606	101.980	101.963	102.037	102.391	102.031	102.705	102.155	101.768	101.278
F	1.704	1.675	1.804	1.756	1.731	1.731	1.740	1.721	1.739	1.734	1.767	1.708	1.709
Na_2O	0.033	0.021	0.054	0.022	0.025	0.032	0.028	0.030	0.022	0.021	0.022	0.026	0.031
MgO	0.000	0.000	0.000	0.000	0.000	0.000	0.000	0.000	0.000	0.000	0.000	0.000	0.000
Al_2O_3	0.000	0.001	0.000	0.000	0.000	0.000	0.000	0.000	0.000	0.000	0.000	0.000	0.000
SiO_2	0.209	0.118	0.052	0.124	0.131	0.159	0.121	0.147	0.125	0.127	0.122	0.157	0.190
P_2O_5	5.841	5.962	6.034	5.947	5.941	5.919	5.968	5.931	5.961	5.943	5.952	5.926	5.900
Cl	0.003	0.002	0.003	0.002	0.002	0.002	0.002	0.002	0.002	0.002	0.002	0.002	0.002
K_2O	0.000	0.000	0.000	0.000	0.000	0.000	0.000	0.000	0.000	0.000	0.000	0.000	0.000
CaO	9.721	9.263	9.661	9.553	9.534	9.504	9.525	9.493	9.561	9.593	9.607	9.498	9.463
TiO_2	0.000	0.000	0.000	0.000	0.000	0.000	0.000	0.000	0.000	0.000	0.000	0.000	0.000
FeO	0.007	0.000	0.008	0.006	0.000	0.000	0.000	0.000	0.000	0.000	0.000	0.000	0.000
SrO	0.117	0.444	0.059	0.190	0.194	0.200	0.166	0.199	0.162	0.170	0.151	0.192	0.191
La_2O_3	0.028	0.035	0.008	0.027	0.031	0.035	0.027	0.037	0.024	0.025	0.023	0.036	0.042
Ce_2O_3	0.044	0.051	0.018	0.045	0.053	0.061	0.049	0.062	0.043	0.043	0.041	0.061	0.073
Pr_2O_3	0.000	0.000	0.000	0.001	0.000	0.000	0.000	0.001	0.000	0.000	0.000	0.001	0.001
Nd_2O_3	0.007	0.008	0.007	0.010	0.013	0.014	0.013	0.015	0.009	0.009	0.008	0.014	0.018
MnO	0.000	0.000	0.006	0.000	0.000	0.000	0.000	0.000	0.000	0.000	0.000	0.000	0.000
Total	17.714	17.579	17.715	17.683	17.655	17.657	17.638	17.637	17.647	17.666	17.695	17.621	17.619
A 2x5	9.950	9.822	9.807	9.848	9.850	9.846	9.807	9.837	9.820	9.861	9.852	9.828	9.820
X 2x3	6.050	6.080	6.086	6.071	6.072	6.078	6.089	6.078	6.086	6.070	6.074	6.083	6.089
Q 2-OH	1.707	1.677	1.807	1.758	1.733	1.733	1.742	1.723	1.741	1.735	1.769	1.710	1.710

Table 4. Analyses of barite grains from carbonatite breccia.

Na_2O	0.122	0.126	0.128	0.129	0.133	0.123	0.126	0.127	0.125	0.118	0.124	0.119
SO_3	32.624	32.857	32.224	31.480	32.203	33.159	32.268	33.283	32.841	32.617	32.886	32.750
CaO	0.012	0.012	0.000	0.000	0.000	0.000	0.000	0.000	0.000	0.000	0.000	0.000
SrO	3.379	4.673	3.124	2.802	3.124	4.018	2.811	3.912	2.487	5.607	3.766	2.699
BaO	64.383	59.630	64.826	60.711	65.419	61.000	61.854	64.275	62.898	58.992	65.209	62.742
La_2O_3	0.000	0.000	0.000	0.000	0.000	0.000	0.000	0.000	0.000	0.000	0.000	0.000
Nd_2O_3	0.000	0.000	0.000	0.000	0.000	0.000	0.000	0.000	0.000	0.000	0.000	0.000
PbO	0.000	0.000	0.000	0.000	0.000	0.000	0.000	0.000	0.000	0.000	0.000	0.000
Ce_2O_3	0.000	0.000	0.000	0.000	0.000	0.000	0.000	0.000	0.000	0.000	0.000	0.000
Total	100.521	97.297	100.312	95.129	100.888	98.301	97.060	101.599	98.357	97.337	101.985	98.312
Na	0.009	0.010	0.010	0.010	0.010	0.009	0.010	0.010	0.010	0.009	0.009	0.009
S	0.972	0.985	0.968	0.980	0.966	0.985	0.982	0.975	0.984	0.980	0.969	0.983
Ca	0.001	0.001	0.000	0.000	0.000	0.000	0.000	0.000	0.000	0.000	0.000	0.000
Sr	0.078	0.108	0.073	0.067	0.072	0.092	0.066	0.089	0.058	0.130	0.086	0.063
Ba	1.001	0.933	1.017	0.987	1.025	0.947	0.983	0.983	0.984	0.925	1.003	0.983
La	0.000	0.000	0.000	0.000	0.000	0.000	0.000	0.000	0.000	0.000	0.000	0.000
Nd	0.000	0.000	0.000	0.000	0.000	0.000	0.000	0.000	0.000	0.000	0.000	0.000
Pb	0.000	0.000	0.000	0.000	0.000	0.000	0.000	0.000	0.000	0.000	0.000	0.000
Ce	0.000	0.000	0.000	0.000	0.000	0.000	0.000	0.000	0.000	0.000	0.000	0.000
Total	2.061	2.036	2.068	2.045	2.073	2.034	2.041	2.056	2.036	2.045	2.067	2.038

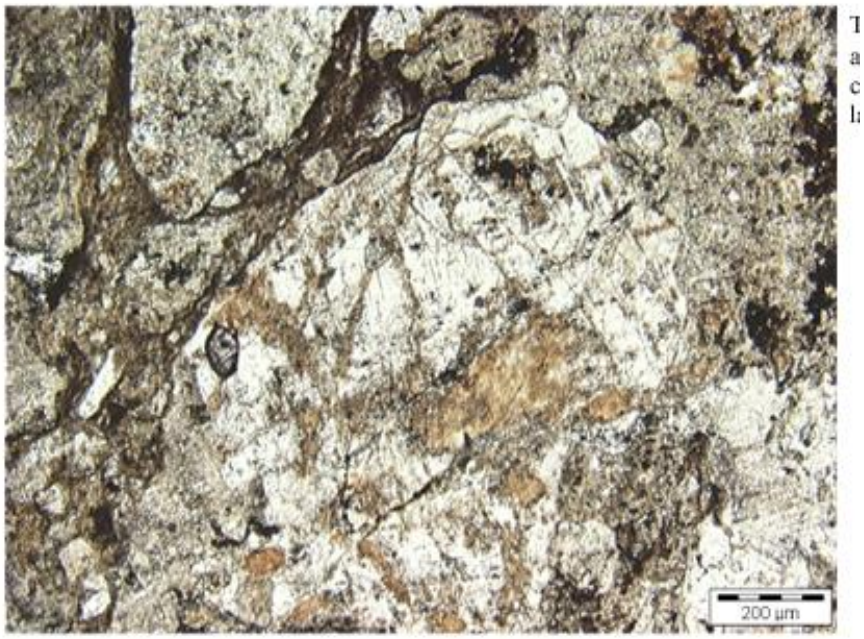

Fig. 10. Zircon within microcline crystal in the carbonatite breccia.

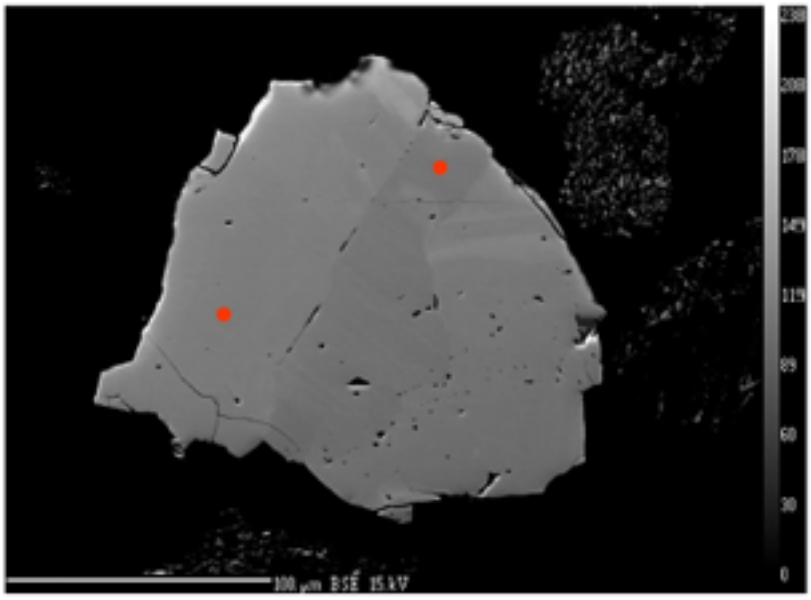

Fig. 11. BSE image of zircon, red dots show points of measurements (darker and lighter sides). Analyses point to an increase in Fe and a decrease in Y, Hf and Th from the lighter domain to the darker domain.

nounced fluctuation is seen in Nb (from core to rim) and this is related to zoning (Fig. 14). Other elements do not show conspicuous fluctuation. Pyrochlore is abundant in Amba Dongar carbonatites and has been studied in detail by Viladkar and Bismayer (2010).

4.7. Thorite

The BSE image (Fig. 15) of thorite contains two mineral domains. Both domains were analysed on EPMA and mineral formulae were calculated for both dark and light parts of the thorite (Table 7). These calculations showed that the general formula could not be used for all measured points. The calculation shows that the lighter part is thorogummite (after Frondel, 1953) with chemical formula of (Th, U) $[(OH,F)_{4x}]$ $(SiO_4)_{1-x}$ and in the darker region the calculated formula is

(Th,U) $[(OH,F)_{0.7}]$ $(SiO_4)_{0.825}$

Table 5. Analyses of zircons from carbonatite breccia.

	Dark	**Light**						
SiO_2	32.781	32.135	33.020	31.992	31.904	31.892	32.874	32.259	32.646
$P2O_5$	0.021	0.027	0.034	0.021	0.068	0.028	0.033	0.095	0.034
CaO	0.000	0.000	0.000	0.000	0.000	0.000	0.014	0.000	0.015
MnO	0.000	0.000	0.000	0.000	0.000	0.000	0.000	0.000	0.000
FeO	0.096	0.000	0.050	0.054	0.049	0.000	0.000	0.083	0.109
$Y2O_3$	0.148	0.356	0.677	0.000	0.249	0.093	0.454	0.214	0.288
ZrO_2	67.591	65.870	68.072	67.269	65.857	67.538	68.521	67.351	67.606
La_2O_3	0.000	0.000	0.000	0.000	0.000	0.000	0.000	0.000	0.000
Ce_2O_3	0.000	0.000	0.000	0.000	0.000	0.000	0.000	0.000	0.000
Nd_2O_3	0.000	0.000	0.000	0.000	0.000	0.000	0.000	0.000	0.000
Gd_2O_3	0.000	0.000	0.000	0.000	0.000	0.000	0.000	0.000	0.000
HfO_2	0.822	0.801	0.815	0.674	1.024	0.441	0.413	0.546	0.609
PbO	0.000	0.000	0.000	0.000	0.000	0.000	0.000	0.000	0.000
ThO_2	0.063	0.581	0.231	0.000	0.756	0.000	0.090	0.573	0.467
U_2O_3	0.000	0.000	0.000	0.000	0.000	0.000	0.000	0.000	0.000
Total	101.560	99.834	102.984	100.034	99.985	100.111	102.481	101.183	101.792
SiO_2	0.992	0.993	0.990	0.984	0.987	0.981	0.988	0.984	0.989
P_2O_5	0.000	0.000	0.001	0.000	0.001	0.000	0.001	0.002	0.001
CaO	0.000	0.000	0.000	0.000	0.000	0.000	0.000	0.000	0.000
MnO	0.000	0.000	0.000	0.000	0.000	0.000	0.000	0.000	0.000
FeO	0.002	0.000	0.001	0.001	0.001	0.000	0.000	0.002	0.003
Y_2O_3	0.001	0.003	0.005	0.000	0.002	0.001	0.004	0.002	0.002
ZrO_2	0.997	0.993	0.995	1.009	0.994	1.013	1.004	1.001	0.998
La_2O_3	0.000	0.000	0.000	0.000	0.000	0.000	0.000	0.000	0.000
Ce_2O_3	0.000	0.000	0.000	0.000	0.000	0.000	0.000	0.000	0.000
Nd_2O_3	0.000	0.000	0.000	0.000	0.000	0.000	0.000	0.000	0.000
Gd_2O_3	0.000	0.000	0.000	0.000	0.000	0.000	0.000	0.000	0.000
HfO_2	0.007	0.007	0.007	0.006	0.009	0.004	0.004	0.005	0.005
PbO	0.000	0.000	0.000	0.000	0.000	0.000	0.000	0.000	0.000
ThO_2	0.000	0.004	0.002	0.000	0.005	0.000	0.001	0.004	0.003
$U2O_3$	0.000	0.000	0.000	0.000	0.000	0.000	0.000	0.000	0.000
Total	2.001	2.000	2.001	2.000	1.999	1.999	2.000	1.999	2.001

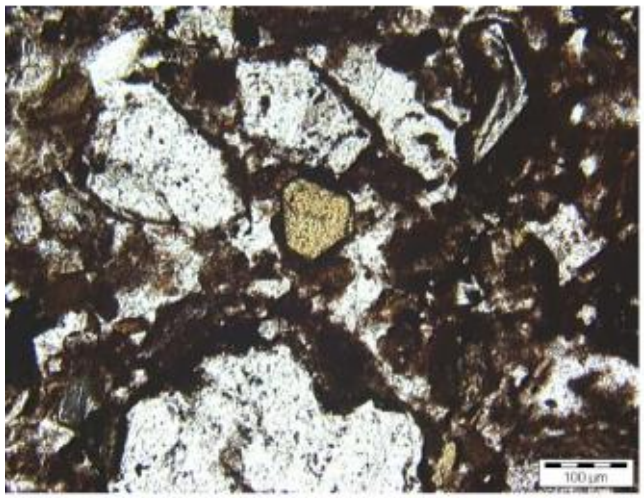

Fig. 12. Shows an idiomorphic pyrochlore in a matrix of carbonatite-breccia. The sample is from the southern part of the ring of breccia.

The presence of different domains in a single crystal was developed due to post-magmatic alteration and this is responsible for the transformation of thorite to thorogummite. The decrease in Th, increase in Ca and also substitution of SiO_4 through fluorine and OH in the analyses of light and dark domains support this conclusion (Lumpkin and Chakoumakos, 1988).

5. Discussion

The most voluminous carbonatite formation, at present level of erosion, in Amba Dongar carbonatite diatreme is the carbonatite breccia. Field observations and the intrusive relations among different carbonatite units support the view of Viladkar (1972, 1981, 1996) that the carbonatite activity in the Amba

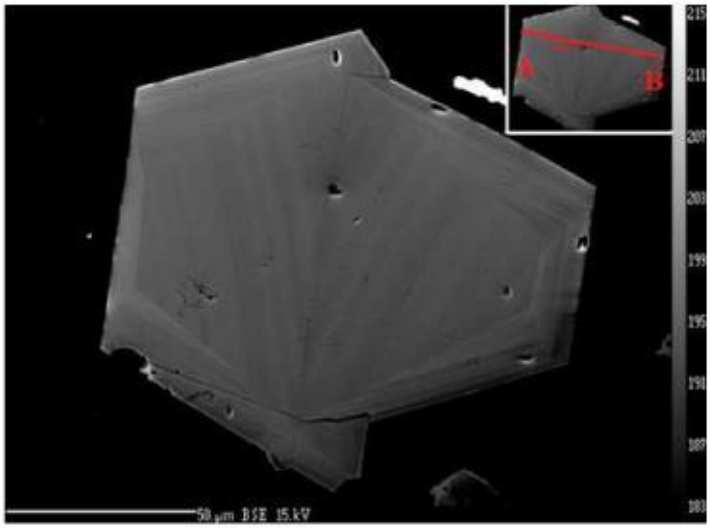

Fig. 13. BSE image of primary zoned and twinned pyrochlore (the inset shows the position of a line scanned with 50 analysed points).

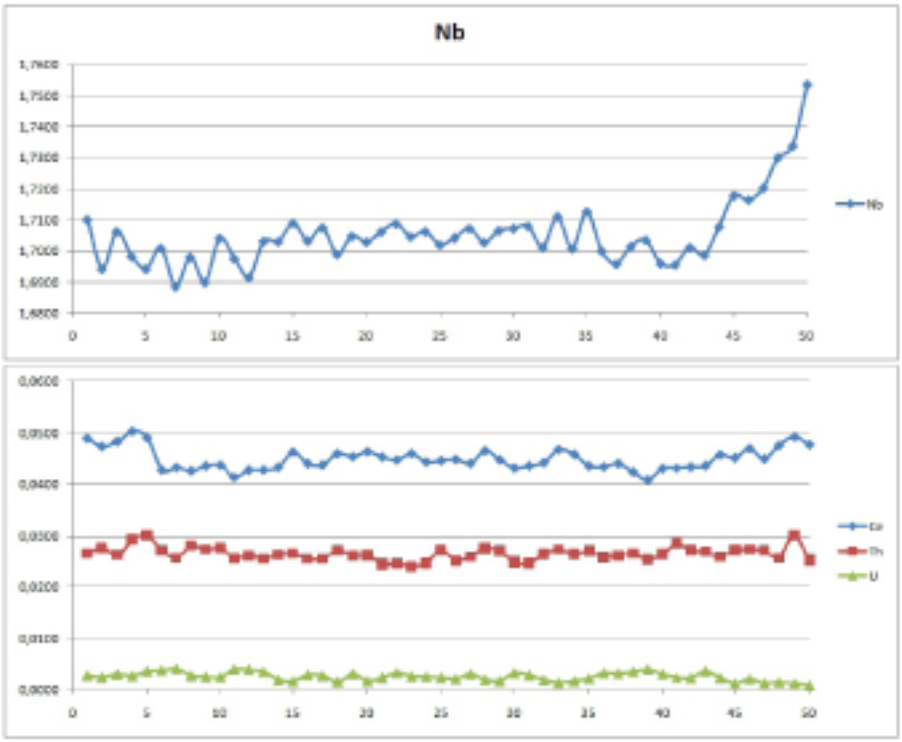

Fig. 14. The elements Nb, U, Th and Ce (atom per formula unit) for each analysed point (plot of A-left to B-right). The plot indicates zoning, especially, the fringe at the right-hand side is affected by fluctuation in Nb.

Dongar started with the emplacement of voluminous carbonatite breccia plug occupying a large area of the diatreme and is considered as a major event in the emplacement of carbonatite diatreme rocks in Amba Dongar. The size of different fragments varies largely and the maximum size reaches more than a meter at times. Most of the sövite fragments, being softer than silicate rocks, are perfectly rounded while the fragments of hard rocks (gneiss, sandstone, basalt, alkaline rocks) tend to be more semi-angular. This breccia was successively invaded by alvikite (phase I), sövite, ankeritic carbonatite, hydrothermal fluorite and quartz veins.

Except for zircon (from metamorphic rock frag-

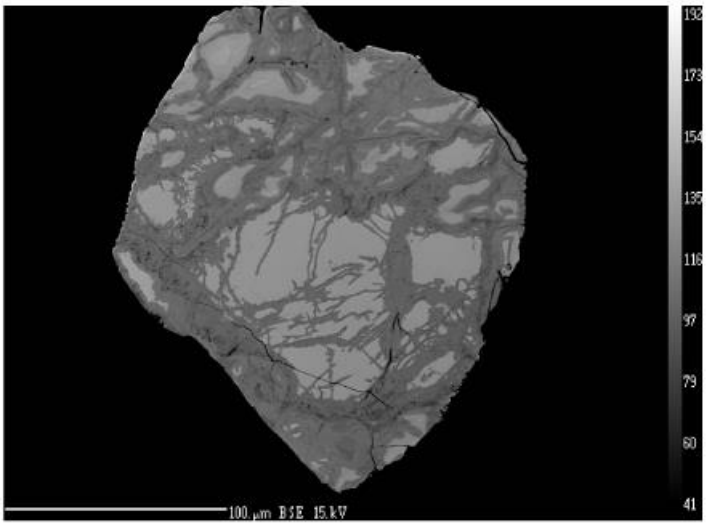

Fig. 15. BSE image of thorite (lighter domain) and alteration to thorogummite (darker domain) with clear visible fission tracts in the central part of the crystal.

Table 6. Pyrochlore analyses from carbonatite breccia.

	Light	Dark		Light	Dark
F	3.766	5.495	Ta	0.000	0.000
Na_2O	4.856	6.040	Ti	0.418	0.264
MgO	0.000	0.026	Nb	1.529	1.664
SiO_2	0.048	0.881			
CaO	17.986	18.723	ΣB=2.0	0.1	0.1
FeO	0.281	0.290			
SrO	0.382	0.736	Na	0.569	0.699
ZrO_2	2.011	1.402	Mg	0.000	0.002
BaO	0.000	0.000	Ca	1.165	1.197
La_2O_3	0.458	0.242	Fe	0.014	0.014
Ce_2O_3	2.721	0.604	Sr	0.013	0.025
Nd_2O_3	0.481	0.095	Ba	0.000	0.000
SmO	0.000	0.000	La	0.010	0.005
Ta_2O_5	0.000	0.000	Ce	0.060	0.013
PbO	0.000	0.000	Nd	0.010	0.002
ThO_2	4.354	0.189	Sm	0.000	0.000
U_2O_3	0.000	0.000	Pb	0.000	0.000
TiO_2	9.187	5.886	Th	0.060	0.003
Nb_2O_5	55.947	61.694	U	0.000	0.000
Total	102.476	102.300			
			A Position	1.888	1.947
Ta/(Ta + Nb)	0.000	0.000	m (bei A)	0.112	0.053
			F	0.720	1.037
Si	0.003	0.053	O	6.500	6.500
Zr	0.059	0.041			

ment) and pyrochlore (sövite fragment of first generation), all other minerals (apatite, barite, thorite) have been incorporated in carbonatite breccia by later intrusives of alvikite, sövite and ankeritic carbonatite. Much of the fluorite and quartz were introduced by invading hydrothermal solutions. Pyrochlore found in sövite xenoliths appears as very fresh and not altered as shown earlier by Viladkar and Bismayer (2010). Both grains show high F and Na which points also to their primary character. UO_2 is not detected in both grains though ThO_2 is reasonably high in one grain. Usually, U and Th concentrations induce metamictization in pyrochlore. In the present case, though one grain has reasonably high Th, it has not induced metamictization in the grain.

Since the carbonatite breccia has been invaded by several pulses of carbonatites, the original matrix is not available for investigation. This is reflected in the trace element (Ba, Sr, Nb, Zr, Th and LREE) concentrations of the matrix, which is very similar to the different carbonatite units of Amba Dongar. Rubidium concentration is high in some matrix samples, and this can be attributed to the presence of fine orthoclasite fragments in the matrix. Unfortunately, not much concentration of REE minerals is noticed though monazite and bastanaesite are found in some samples. Some breccia outcrops are affected by hydrothermal solutions carrying fluorite, barite and quartz; however, these minerals need to be studied in detail for possible REE mineralization.

The rounded nature of fragments indicates that the process of fluidization was responsible for the formation of carbonatite-breccia. Continuous churning under high CO_2 pressure was perhaps the reason for rounded fragments (Viladkar, 1972). As for the emplacement of carbonatite breccia, the present study assumes the presence of calcio-carbonatite magma at depth which induced fenitization of the protolith metamorphic rocks and Bagh sandstone. In later stages, high CO_2 pressure may have initiated the process of fluidization and the emplacement of carbonatite breccia. A similar mechanism of fluidization process was proposed for Chilwa Island in Malawi

Table 7. Analyses of thorites.

F	0.000	0.183	0.000	0.000	0.000	1.043	0.509	0.746	0.731	0.780	0.819	1.185
SiO_2	19.163	18.374	18.960	18.635	18.851	18.227	17.823	17.838	18.413	17.953	18.147	17.525
CaO	0.000	0.000	0.000	0.000	0.000	0.597	0.044	0.523	0.033	0.291	0.000	1.139
ThO_2	80.251	78.234	79.237	78.508	78.983	76.964	76.620	74.676	76.807	75.989	77.966	73.479
$U2O_3$	0.832	0.688	0.612	0.520	0.677	0.605	0.588	0.537	0.701	0.680	0.603	0.612
Total	100.253	97.478	98.955	97.731	98.511	97.436	95.583	94.320	96.685	95.692	97.551	93.940
F	0.000	0.032	0.000	0.000	0.000	0.183	0.091	0.134	0.129	0.139	0.144	0.215
SiO_2	1.022	1.014	1.024	1.020	1.022	1.009	1.009	1.015	1.024	1.013	1.010	1.004
CaO	0.000	0.000	0.000	0.000	0.000	0.035	0.003	0.032	0.002	0.018	0.000	0.070
ThO_2	0.974	0.983	0.974	0.978	0.975	0.970	0.987	0.967	0.972	0.975	0.987	0.958
U_2O_3	0.005	0.004	0.004	0.003	0.004	0.004	0.004	0.004	0.004	0.004	0.004	0.004
Total	2.001	2.033	2.001	2.001	2.001	2.201	2.093	2.151	2.131	2.149	2.145	2.251

(Smith, 1956) and Blackburn carbonatite in Ottawa (Hogarth and Rushforth, 1988). The formation of such breccia seems to have involved much stress and explosion. There seem some similarities between Amba Dongar breccia and 'explosion breccia' described by Clement (1982) in kimberlite pipes. Chandra et al. (2022) presented the geochemical analyses of breccias along with other carbonatite units. However, a detailed mineralogy of the carbonatite breccias is lacking in that work.

6. Conclusions

Carbonatite breccia is a very important unit of the carbonatite ring structure in the Amba Dongar carbonatite ring complex. Its origin and emplacement history has been discussed by Viladkar (1981). The present study shows that the breccia unit of carbonatite in the ring structure is very important for the detailed investigation of economic mineralization. Pyrochlore, apatite, barite, thorite and fluorite occur in reasonably good concentrations in different sections in this rock unit.

ACKNOWLEDGEMENTS

We thank Stefani Heidrich, Mineralogisch-Petrographisches Institute of the University of Hamburg for technical assistance on the EPMA, and Peter Stutz for polished EPMA sections. We are grateful to Liu Yan, Chinese Academy of Geological Sciences, Beijing, for his comments and suggestions on the paper.

References

Chandra, J., Paul, D., Uniyal, A., 2022. Petrography and geochemistry of carbonatite breccia from Amba Dongar carbonatite complex, Gujarat in the Deccan Large Igneous Province suggest mantle origin. *Journal of Earth System Science* 131(2). https://doi.org/10.1007/s12040-022-01861-w.

Clement, C.R., 1982. *A Comparative Geological Study of some Major Kimberlite Pipes in the Northern Cape and Orange Free State.* Phd thesis. University of Cape Town. South Africa.

Doroshkevich, A.G., Viladkar, S.G., Ripp, G., Burtseva, M., 2009. Hydrothermal REE mineralization in the Amba Dongar carbonatite complex, Gujarat, India. *Canadian Mineralogist* 47, 1105–1116. https://doi.org/10.3749/canmin.47.5.1105.

Frondel, C., 1953. Hydroxyl substitution in thorite and zircon. *American Mineralogist: Journal of Earth and Planetary Materials* 38(11-12), 1007–1018.

Geisler, T., Schaltegger, U., Tomaschek, F., 2007. Re-equilibration of zircon in aqueous fluids and melts. *Elements* 3, 43–50. https://doi.org/10.2113/gselements.3.1.43.

Gittins, J., 1989. Carbonatite origin and diversity. *Nature* 338.

Hogarth, D.D., Rushforth, P., 1988. The Blackburn carbonatites, near Ottawa, Ontario: Dykes with fluidized emplacement. *Canadian Mineralogist* 26, 377–390.

Lumpkin, G.R., Chakoumakos, B.C., 1988. Chemistry and radiation effects of thorite-group minerals from the Harding pegmatite, Taos County, New Mexico. *American Mineralogist* 73, 1405–1419.

Smith, W.C., 1956. Review of some problems of African carbonatites. *Quart. J. Geol. Soc. London* 112, 189–219.

Sukheswala, R.N., Viladkar, S.G., 1981. Fenitized sand¬stones in Amba Dongar carbonatites, Gujarat, India. *Jour. Geol. Soc. India* 22, 368–374.

Viladkar, S.G., 1972. *Geology of the Amba Dongar Carbonatite-alkalic complex, Gujarat.* Ph.d. thesis. University of Bombay.

Viladkar, S.G., 1981. The carbonatites of Amba Dongar, Gujarat, India. *Bull. Geol. Soc. Finland* 53, 17–28.

Viladkar, S.G., 1986. Fenitization at the Amba Dongar carbonatite-alkalic complex, India, in: Proceedings, NEMI-RAM Sympos¬ium, Czechoslovakia, p. 172–189.

Viladkar, S.G., 1996. *Geology of the Carbonatite-alkalic Diatreme of Amba Dongar, Gujarat.* GMDC Science and Research Centre, Ahmedabad.

Viladkar, S.G., Bismayer, U., 2010. Compositional variation in pyrochlores of Amba Dongar Carbonatite Complex, Gujarat. *J. Geol. Soc. India* 75, 495–502. https://doi.org/10.1007/s12594-010-0048-2.

Appendix tables: EPMA analytical conditions used for the analysis of thorite, zircon, barite, and apatite

Table A. Analytical condition for thorite with 15 keV und 20 nA.

Element	Line	Crystal	Standard	Peak cnt time (s)	Bg cnt time (s)	Detection limit (wt%)
F	Ka	TAP	LiF	60	30	0.1590
Si	Ka	TAP	Th-Glas	20	10	0.0315
Ca	Ka	PET	Andradit	60	30	0.0232
Th	Mb	PET	Th-Glas	30	15	0.4274
U	Mb	PET	UO_2	60	30	0.1831

Table B. Analytical conditions for zircon with 15 keV und 50 nA.

Element	Line	Crystal	Standard	Peak cnt time (s)	Bg cnt time (s)	Detection limit (wt%)
Al	Ka	TAP	Al_2O_3	60	30	0.0069
Si	Ka	TAP	$ZrSiO_4$	20	10	0.0133
P	Ka	LPET	Apatit	60	30	0.0072
Ca	Ka	PET	Andradit	60	30	0.0115
Mn	Ka	LIF	$MnTiO_3$	60	30	0.0300
Fe	Ka	LIF	Andradit	60	30	0.0331
Y	La	LPET	Y_2O_3	60	30	0.0245
Zr	La	PET	$ZrSiO_4$	20	10	0.0961
La	La	LPET	REE3	60	30	0.0215
Ce	La	LPET	REE2	60	30	0.0220
Nd	Lb	LPET	REE4	60	30	0.0485
Gd	La	LIF	Gd	60	30	0.0889
Hf	La	LIF	Hf	60	30	0.1359
Pb	Ma	LPET	Pb-Glas	60	30	0.0372
Th	Ma	LPET	Th-Glas	60	30	0.0315
U	Mb	LPET	UO_2	60	30	0.0439

Table C. Analytical conditions for barite with 15 keV und 50 nA.

Element	Line	Crystal	Standard	Peak cnt time (s)	Bg cnt time (s)	Detection limit (wt%)
Na	Ka	TAP	Albit	60	30	0.0127
S	Ka	PET	$BaSO_4$	20	10	0.0229
Ca	Ka	PET	Andradit	60	30	0.0116
Sr	La	PET	$SrTiO_3$	60	30	0.0385
Ba	La	PET	$BaSO_4$	20	10	0.0872
La	La	LPET	REE3	60	30	0.0255
Nd	Lb	LPET	REE4	60	30	0.0811
Pb	Ma	LPET	Pb-Glas	60	30	0.0884
Ce	Lb	LPET	REE2	60	30	0.0623

Table D. Analytical conditions for apatite with 15 keV and 50 nA.

Element	Line	Crystal	Standard	Peak cnt time (s)	Bg cnt time (s)	Detection limit (wt%)
F	Ka	TAP	Apatit	60	30	0.0134
Na	Ka	TAP	Albit	60	30	0.0104
Mg	Ka	TAP	MgO	60	30	0.0072
Al	Ka	TAP	Al_2O_3	60	30	0.0065
Si	Ka	TAP	Andradit	60	30	0.0074
P	Ka	TAP	Apatit	10	5	0.0269
Cl	Ka	LPET	Vanadinit	60	30	0.0051
K	Ka	PET	Orthoklas	60	30	0.0085
Ca	Ka	PET	Apatit	10	5	0.0299
Ti	Ka	PET	$MnTiO_3$	60	30	0.0141
Fe	Ka	LIF	Andradit	60	30	0.0288
Sr	La	PET	$SrTiO_3$	60	30	0.0289
La	La	LPET	REE3	120	60	0.0134
Ce	La	LPET	REE2	120	60	0.0138
Pr	Lb	LPET	REE1	120	60	0.0307
Nd	Lb	LPET	REE4	120	60	0.0311
Mn	Ka	LIF	$MnTiO_3$	60	30	0.0268